

Projections of seasonal patterns in temperature-related deaths for Manhattan, New York

Tiantian Li¹, Radley M. Horton² and Patrick L. Kinney³*

Global average temperatures have been rising for the past half-century, and the warming trend has accelerated in recent decades¹. Further warming is expected over the next few decades, with significant regional variations. These warming trends will probably result in more frequent, intense and persistent periods of hot temperatures in summer, and generally higher temperatures in winter. Daily death counts in cities increase markedly when temperatures reach levels that are very high relative to what is normal in a given location^{2–4}. Relatively cold temperatures also seem to carry risk^{2,4}. Rising temperatures may result in more heat-related mortality but may also reduce cold-related mortality, and the net impact on annual mortality remains uncertain. Here we use 16 downscaled global climate models and two emissions scenarios to estimate present and future seasonal patterns in temperature-related mortality in Manhattan, New York. All 32 projections yielded warm-season increases and cold-season decreases in temperature-related mortality, with positive net annual temperature-related deaths in all cases. Monthly analyses showed that the largest percentage increases may occur in May and September. These results suggest that, over a range of models and scenarios of future greenhouse gas emissions, increases in heat-related mortality could outweigh reductions in cold-related mortality, with shifting seasonal patterns.

The impact of warming temperatures on population health is of increasing concern to health practitioners and policymakers. There is an urgent need for studies that assess temperature-related mortality risks over the full year under present and projected future climates. Such studies can lead to improved understanding of weather and climate vulnerability in the health sector, and more informed risk management and adaptation decisions. Urban areas such as New York City are especially vulnerable to temperature extremes owing to the high concentration of susceptible populations⁵, as well as enhancement of temperatures due to the urban heat island effects⁶. Temperatures in the New York City region increased by 2 °C between 1901 and 2000 (ref. 5), substantially exceeding global and US national trends⁷. Preparing for and preventing temperature-related health problems has been identified as a high priority topic by New York City's government⁸.

Several studies have projected future heat-related mortality resulting from climate change^{9–14}. These studies follow a health impact assessment approach, integrating temperature projections from global-scale climate models with empirical exposure–response relationships from the epidemiologic literature. Although most health impact assessments for climate change have focused on heat-related mortality, decreasing cold-related mortality may also

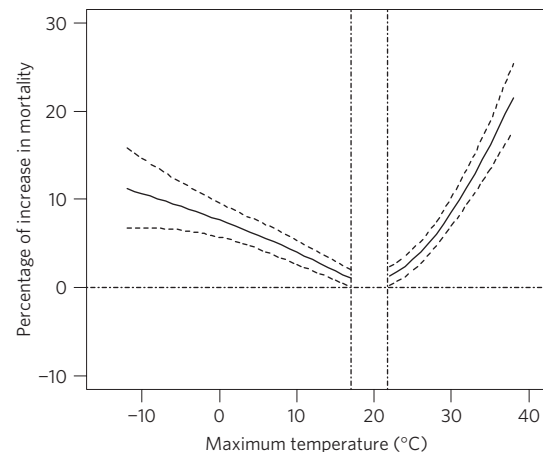


Figure 1 | Exposure–response curve for temperature-related mortality.

The solid line shows the central estimates. The dashed line shows the 95% confidence intervals.

be important¹⁵. A growing number of studies have examined seasonal mortality tradeoffs in a changing climate^{16–22}. However, results have been difficult to compare owing to differences in health and climate modelling methods. The objective of the present study was to project future temperature-related mortality impacts over the full year for the NYC borough of Manhattan (New York County) across a broad range of statistically downscaled climate models and greenhouse gas emissions scenarios in the 2020s, 2050s and 2080s.

Fitted spline functions relating percentage increase in daily mortality to daily T_{\max} in °C using historical data are shown graphically in Fig. 1. The warm and cold portions of the function were fitted separately at lag 0 and 2, respectively (see Supplementary Equation 1 and Figs S1–S2). Both cold and hot deviations from a central range were associated with excess mortality. A healthy temperatures range, that is, temperatures for which there was no statistically significant temperature effect, extended from 17.2 to 21.7 °C (Fig. 1). Results were not affected substantially in sensitivity models that included ozone, particulate matter with aerodynamic diameter of 10 μm or less (PM_{10}), dewpoint temperature or an indicator for influenza epidemics (Supplementary Tables S4–S7). We linked the exposure–response function shown in Fig. 1 to 32 modelled projections of daily temperatures (see Methods and Supplementary Table S1) to estimate the numbers of temperature-related deaths in both the baseline and future time periods as described below.

¹Institute for Environmental Health and Related Product Safety, Chinese Center for Disease Control and Prevention, Beijing 100050, China, ²Center for Climate Systems Research, Columbia University, New York 10025, USA, ³Mailman School of Public Health, Columbia University, New York 10032, USA.

*e-mail: plk3@columbia.edu

Table 1 | Percentage change in annual heat-related, cold-related and net deaths in the 2020s, 2050s and 2080s as compared with the 1980s.

Scenario	GCMs	2020s			2050s			2080s		
		Net	Heat*	Cold†	Net	Heat*	Cold†	Net	Heat*	Cold†
B1	BCCR	0.9	11.3	-10.2	3.5	20.8	-15.3	10.4	37.8	-19.3
	CCSM	4.8	24.5	-16.7	6.7	33.7	-22.6	9.4	35.6	-19.0
	CGCM	7.7	23.9	-9.9	10.5	38.1	-19.5	16.5	52.2	-22.2
	CNRM	3.9	17.7	-11.1	8.8	30.6	-14.9	12.4	40.8	-18.4
	CSIRO	0.4	14.0	-14.3	4.7	23.5	-15.8	6.3	30.9	-20.5
	ECHAM5	4.7	17.7	-9.5	10.9	36.7	-17.1	21.2	61.9	-22.9
	ECHO-G	10.9	30.8	-10.7	16.5	49.0	-18.9	23.8	69.7	-26.0
	GFDL-CM2.0	12.0	32.4	-10.1	20.3	52.8	-15.0	20.5	59.1	-21.5
	GFDL-CM2.1	6.8	24.8	-12.7	15.3	44.7	-16.5	18.8	55.4	-20.9
	GISS	4.4	17.6	-10.0	5.2	20.3	-11.2	8.0	27.3	-12.9
	INMCM	9.4	29.0	-11.8	15.8	44.0	-14.8	15.9	50.0	-21.2
	IPSL	3.9	23.1	-16.9	11.9	45.5	-24.5	19.8	67.1	-31.7
	MIROC	6.0	25.4	-15.1	14.2	46.8	-21.3	19.5	63.9	-28.6
	MRI	1.6	14.0	-11.8	7.8	27.3	-13.4	9.9	37.8	-20.3
	PCM	4.4	19.7	-12.3	7.7	28.4	-14.8	12.1	39.3	-17.4
	UKMO-HadCM3	3.6	18.2	-12.3	15.2	48.7	-21.2	22.7	71.5	-30.4
	Mean	5.3	21.5	-12.2	10.9	36.9	-17.3	15.5	50.0	-22.1
A2	BCCR	0.9	10.1	-9.1	7.7	34.0	-21.0	19.8	65.0	-29.3
	CCSM	5.7	23.7	-13.8	15.7	54.6	-26.5	29.5	90.8	-37.0
	CGCM	7.8	26.0	-11.9	16.2	53.1	-23.9	33.7	99.9	-38.3
	CNRM	5.7	19.4	-9.3	13.3	42.4	-18.2	28.4	81.9	-29.6
	CSIRO	2.2	16.5	-13.4	6.2	34.0	-23.9	16.0	64.0	-36.0
	ECHAM5	2.8	12.7	-7.9	14.6	45.5	-19.0	31.8	89.6	-30.9
	ECHO-G	9.3	29.7	-12.7	19.4	60.2	-24.8	38.1	107.0	-36.7
	GFDL-CM2.0	12.3	32.0	-9.0	24.2	67.6	-22.9	48.2	125.2	-35.4
	GFDL-CM2.1	8.6	26.0	-10.2	17.1	51.1	-19.9	34.6	96.0	-32.2
	GISS	4.0	14.1	-7.0	8.0	30.8	-16.7	16.4	58.2	-28.8
	INMCM	10.3	32.7	-14.0	19.5	57.5	-21.8	37.0	100.7	-32.2
	IPSL	4.5	24.1	-16.7	15.5	57.7	-30.3	32.6	104.8	-45.9
	MIROC	7.1	26.0	-13.5	17.2	57.0	-26.0	35.2	109.0	-44.9
	MRI	2.4	12.7	-8.8	16.2	45.5	-15.5	32.3	89.6	-30.0
	PCM	6.4	22.3	-10.9	11.0	34.5	-14.5	16.8	55.0	-24.7
	UKMO-HadCM3	9.7	26.9	-8.9	24.2	64.4	-19.6	45.8	119.5	-34.2
	Mean	6.2	22.2	-11.1	15.4	49.4	-21.5	31.0	91.0	-34.1

*Percentage changes relative to 1980s annual heat-related deaths of 369. †Percentage changes relative to 1980s annual cold-related deaths of 340.

Table 1 reports the percentage changes in estimated temperature-related deaths for the 2020s, 2050s and 2080s as compared with estimated deaths in the 1980s. Results are presented separately for the A2 and B1 scenarios, and for each of the 16 climate models. More detailed results are provided in Supplementary Table S2. For all 16 models and both emissions scenarios, increasing heat-related deaths, and decreasing cold-related deaths, were projected for future decades. In all cases however, net annual deaths increased in future decades. Under the B1 scenario, net annual temperature-related deaths increased on average by 5.3% (range across models: 0.4–12.0%) in the 2020s, 10.9% (3.5–20.3) in the 2050s, and 15.5% (6.3–23.8) in the 2080s, all compared with a climate baseline in the 1980s. Larger increases were seen for the A2 scenario, especially in the 2050s and 2080s. Net temperature-related additional mortality projections from the GFDL-CM2.0 model increased most markedly from the 1980s to 2080s among all 16 models under both scenarios. Increases projected by the CSIRO model were lowest.

Figure 2 graphically summarizes the annual net temperature-, heat- and cold-related deaths from the 1980s to 2080s. Net

temperature- and heat-related deaths under the A2 scenario increased more rapidly from the 1980s to 2080s compared with the B1 scenario.

Impacts on mortality of future warming varied substantially across months (Fig. 3 and Supplementary Figs S3 and S4). Monthly analyses showed that the largest absolute changes occurred in summer and winter (Supplementary Fig. S3). However, percentage increases in temperature-related deaths in the 2080s were largest in the months of May and September, with about a 100% increase for the A2 scenario. Similar patterns across months were observed for the other decades and for the B1 scenario (Supplementary Fig. S4).

This study is the first to apply downscaled climate projections from a full suite of available models to investigate how climate change may affect future annual temperature-related deaths, accounting for both heat and cold effects on mortality. Across this broad range of models, we projected increasing annual temperature-related deaths for Manhattan County in the 2020s, 2050s and 2080s.

Several previous studies have projected increases in future heat-related deaths in a warming climate^{9–14}; others have assessed

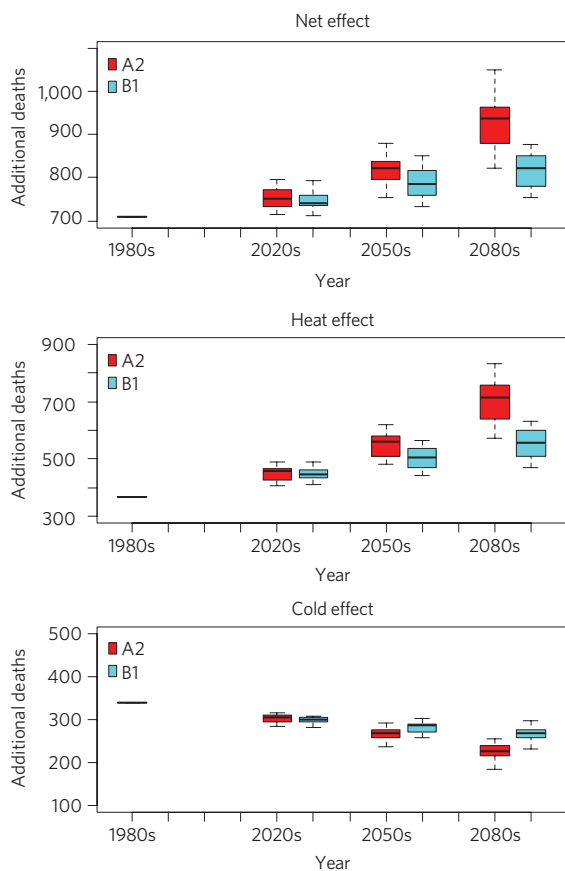


Figure 2 | Distribution of heat-related, cold-related and net annual temperature-related deaths in the 1980s, 2020s, 2050s and 2080s for 16 climate models and the A2 and B1 greenhouse gas scenarios. The box symbols represent, from bottom to top, the minimum, 25th percentile, 50th percentile, 75th percentile and maximum across 16 models.

the extent to which decreases in cold-related deaths may offset heat-related deaths^{16–22}. It is difficult to draw general conclusions from the body of work so far because each study used one or a small number of different climate models/scenarios. Here, we estimated mortality effects across a full range of available downscaled climate models as well as both high and low greenhouse gas scenarios. One consistent finding from previous work is that estimated mortality benefits due to warming winters are substantially smaller in studies that controlled thoroughly for seasonal effects when analysing observed exposure–responses^{17,18,20}, than in those that did not^{19,21,22}. We too avoided winter-season confounding by controlling for seasonality in our analysis of observed temperature–mortality associations. Finally, ours is the first study to report climate-change projections of monthly mortality.

We developed an empirical exposure–response relationship for temperature-related mortality in Manhattan using observed data from the baseline period. We explored lags from 0 to 5 days, and determined that heat-related mortality was best predicted using same-day temperature, whereas cold-related mortality was better predicted by lag-2 temperature. This is consistent with previous epidemiology studies, which have typically applied lags of 0–3 days for heat effects, and lags of 2–5 days for cold effects^{2,23,24}. Recently ref.⁴ fitted cold-related mortality with a 25-day moving average of previous temperatures in a multi-city analysis. However, this long distributed lag probably captured seasonal elevations in mortality, and thus is difficult to interpret as a direct effect of cold temperatures. In sensitivity analyses, we examined single-day and cumulative lags of 5 and 10 days. The heat effect was slightly

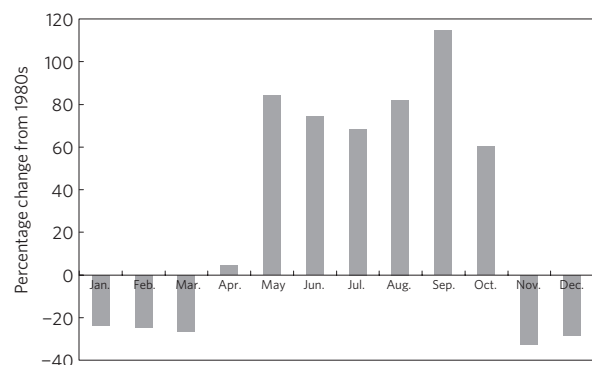


Figure 3 | Percentage change (average over 16 models) in monthly temperature-related deaths in the 2080s versus the 1980s for the A2 scenario. The largest percentage changes are seen for the months of May and September.

higher using a 2-day moving average. Neither the 5- nor 10-day moving average had a statistically significant effect on cold-season mortality, and the effect estimates were not dissimilar to that at lag 2 in our core analysis.

We used Poisson general linear regression analysis with natural splines to characterize the nonlinear relationships between daily maximum temperature and daily death counts using observations from 1982 to 1999. This captured the nonlinear nature of temperature effects on mortality. Recent studies have used a more flexible nonlinear modelling approach based on the distributed lag nonlinear package in R (refs 14,25,26). To verify our approach, in sensitivity analyses we used the distributed lag nonlinear model to fit nonlinear temperature effects up to a maximum lag of 30 days (Supplementary Information). Findings confirmed that the heat effect was maximal at lag 0 and diminished rapidly beyond lag 2. The cold effect was distributed over lags 1–4, and maximal at lag 2. We defined a healthy temperature range from 17.2 to 21.7 °C within which no excess mortality due to temperature was assumed to occur. As the healthy range was defined on the basis of statistical significance, it is important to note that this range is sensitive to sample size and cannot be directly compared across locations with different population sizes.

This study used downscaled projections from 16 different global climate models and two greenhouse gas emissions scenarios to project future-year temperature-related deaths, providing an ensemble of future mortality estimates. Estimated annual mortality impacts from the different models/scenarios were similar in the 2020s, but began to diverge in the 2050s and differed substantially by the 2080s. The pattern of divergence in mortality mirrors a similar pattern of divergence in projected warming; greenhouse gas concentrations associated with B1 and A2 diverge as the century progresses (the greenhouse gas emissions trajectories diverge quite rapidly, but the signature in temperatures is delayed owing both to the long residence time of many greenhouse gases and the large inertia of the climate system), and the uncertainty associated with estimates of climate sensitivity has an increasing effect on temperature projections as greenhouse gas concentrations rise. Generating results from a broad range of models and multiple emissions scenarios provides uncertainty information for policymakers concerned with adaptation planning for climate change and health.

Our full-year analysis made it possible to examine changes in temperature-related mortality by calendar month. Large percentage increases in mortality occurred in the months surrounding summer, that is, May and September (Fig. 3), when absolute mortality associated with temperature is relatively low at present. This finding suggests that adaptation planning strategies for the

public health sector may require promoting awareness among the public and practitioners about the need for vigilance outside the traditional high-heat-risk months of June–August.

Several sources of uncertainty are encountered in estimating future health impacts, including those related to climate, health impacts and populations. To address climate uncertainties, we included all 16 climate models available for two greenhouse gas scenarios under a statistically downscaled product. We chose the 1980s as our modelling baseline because this decade is at the centre of the conventional climatological baseline period of 1970–1999. To reduce health impact uncertainties, the exposure–response curves used to project future impacts were developed using observations from the same city in which projections were modelled. However, we assumed a constant population from year 2000 Census data for our calculations of temperature-related mortality. Increasing total population or proportion of vulnerable subpopulations (for example, older adults) would increase the absolute number of temperature-related deaths in the future. In this sense, our method may give conservative projections of future mortality effects as the population of NYC is expected to rise and age for several decades. Changes in other factors that influence population vulnerability, such as general health, access to health care, socio-economic status and exposure to public health messaging are more uncertain.

We did not take into account the possible effects of future adaptation to warmer temperatures by the at-risk population. The use of air-conditioning, heat alerts and cooling shelters as well as gradual physiological adaption could ameliorate significantly the exposure to heat stress¹¹. However, not all vulnerable people have access to air-conditioning. Adaptation would be expected to diminish the magnitude of future mortality response to summer temperatures. On the other hand, there is evidence that mortality related to cold temperatures is enhanced in cities with warm climates, which would tend to reduce the cold-related mortality benefits we projected here^{3,4}. By ignoring these adaptation phenomena, we may have overestimated both heat-related increases and cold-related decreases under future climates, with uncertain net effects. Other factors not considered here because they are considered more uncertain than temperature projections include possible changes in humidity (which together with temperature defines heat stress indices), and how air quality may be affected by climatic factors including warming and changes in atmospheric circulation.

Methods

As described in detail below, we first estimated the exposure–response relationship between observed daily mortality and temperature data in Manhattan. We then obtained downscaled future temperature projections from 16 climate models and two greenhouse gas emissions scenarios for Manhattan. These two inputs were combined to estimate future mortality related to future temperatures, which were compared with temperature-related mortality in a climatological baseline period. We separately accounted for cold-season and warm-season mortality, and also computed net annual changes. Finally, we examined monthly projections of future mortality.

Historical data on daily deaths covering the 1982–1999 period for Manhattan were obtained from the US National Center for Health Statistics. Daily death counts for all internal causes (ICD-9 codes 0-799.9 for 1982–1998 and ICD-10 codes A00-R99 for 1999) were pooled, excluding accidental causes. We chose this definition for consistency with previous studies; however, this would tend to underestimate heat-related mortality because heat stroke is an accidental cause. Daily T_{\max} data were obtained from the National Climatic Data Center for 1982–1999 at the Central Park station.

A statistical model (see Supplementary Equation S1) was developed using Poisson general linear regression with log daily non-accidental death counts as the outcome variable and the following predictors: a spline function of daily T_{\max} with 3 degrees of freedom, a natural spline of time with 7 degrees of freedom per year, and a day of week indicator variable. This approach was similar to that used to study temperature for 11 eastern US communities². Sensitivity analyses investigated potential confounding by ozone, PM_{10} , dewpoint temperature and influenza epidemics. We also tested the robustness of results to the different lag structures. Details are given in Supplementary Tables S3–S7).

Future temperature projections were developed using downscaled outputs from 16 global-scale general circulation models (GCMs) used in the Intergovernmental Panel on Climate Change Fourth Assessment report¹, in conjunction with two future greenhouse gas emissions scenarios²⁷. The approach uses monthly bias-corrected and spatially disaggregated (BCSD) climate projections at 1/8° resolution derived from the WCRP CMIP3 multi-model data set. The BCSD projections were obtained online²⁸. The output from the land-based grid box corresponding to Central Park was used to create change factors for each calendar month based on the difference between each 30-year future time slice and the same GCM's 30-year baseline time slice⁵. These change factors are then applied to the daily Central Park weather data to create a future projection with the same statistical characteristics and sequence as the observations.

The approach described here does not explore how intra-annual and inter-annual temperature variability may change, for several reasons. First, such variability changes are generally considered more uncertain than mean changes²⁹. In addition, the New York City weather station used in this study does not show a significant trend in the variance of either daily summer maximum temperatures or winter minimum temperatures. Further, in an analysis of daily projections for the NYC grid box from three GCMs, it was shown that neither summer T_{\max} nor winter T_{\min} showed significant changes in variance to 2080⁶. By not considering sub-monthly changes in variability, we were able to use fine-spatial-resolution projections (as the 1/8° BCSD product is monthly, not daily) and analyse the entire twenty-first century (whereas using daily data would have constrained the analysis to the 2046–2065 and 2081–2100 time slices for which only a subset (9) of the GCMs are available from the PCMDI data portal). Note that by applying the delta method separately for each calendar month, we do capture one component of possible changes in intra-annual variance, changes in the annual temperature cycle. Previous studies have found changes in the annual cycle to be important³⁰.

This methodology yielded a set of 32 synthetic future temperature projections for daily T_{\max} from 2010 to 2100 based on the three 30-year time slices, and for a baseline period 1970–1999. The 16 GCMs for which BCSD was applied are described in Supplementary Table S1.

Greenhouse gas emissions scenarios represent specific blends of demographic, social, economic, technological and environmental assumptions²⁷. We selected 2 scenarios, A2 and B1, which represent relatively high and low greenhouse gas growth projections, respectively. The A2 scenario assumes relatively rapid population growth and limited sharing of technological change, which combine to produce high greenhouse gas levels by the end of this century, with emissions growing throughout the entire century. The B1 scenario assumes a high level of environmental and social consciousness, which leads to sustainable development, low population growth, high economic and technological advancement, and low energy use. Area devoted to crops and grasslands decreases, whereas reforestation efforts expand forests.

Projected mortality impacts were estimated using modelled daily T_{\max} . For any day with T_{\max} greater than 21.7°C, the change in mortality was calculated relative to the minimum mortality temperature for the heat effect, that is, 15.0°C. For any day with T_{\max} less than 17.2°C, the change in mortality was calculated relative to the minimum mortality temperature for the cold effect, that is, 22.2°C. For days with T_{\max} from 17.2 to 21.7°C, we assumed no temperature effect. Daily additional deaths were computed as

$$\Delta\text{Mortality} = Y_0 \times \text{ERC} \times \text{POP}$$

where $\Delta\text{Mortality}$ is daily temperature-related additional deaths; Y_0 is baseline daily mortality rate (per 100,000 population); POP is county population; ERC is percentage change in mortality for a specified change in temperature, derived from the statistical analysis of observed data as described above.

We computed temperature-related daily deaths in this way for each time period (1980s, 2020s, 2050s, 2080s), and then computed the average number of temperature-related deaths per year (Fig. 2). We also computed percentage changes in annual average deaths from the 1980s to future time periods (Table 1).

The population of Manhattan was based on data obtained from the US census 2000 survey, and was held constant throughout the projection period. Baseline mortality rates for all ages, which excluded deaths attributable to external causes, were obtained from the US Centers for Disease Control and Prevention. We held baseline mortality rates constant in our projection.

Received 19 June 2012; accepted 15 April 2013; published online 19 May 2013

References

1. IPCC *Climate Change 2007: Impacts, Adaptation and Vulnerability* (eds Parry, M. et al.) (Cambridge Univ. Press, 2007).
2. Curriero, F. C. et al. Temperature and mortality in 11 cities of the Eastern United States. *Am. J. Epidemiol.* **155**, 80–87 (2002).
3. McMichael, A. J. et al. International study of temperature, heat and urban mortality: The 'ISOTHURM' project. *Int. J. Epidemiol.* **37**, 1121–1131 (2008).

4. Anderson, B. G. & Bell, M. L. Weather-related mortality: How heat, cold, and heat waves affect mortality in the United States. *Epidemiology* **20**, 205–213 (2009).
5. Rosenzweig, C. *et al.* Responding to climate change in New York State: The climAID integrated assessment for effective climate change adaptation in New York State. *Ann. NY Acad. Sci.* **1244**, 2–649 (2011).
6. Horton, R. M. *et al.* Climate hazard assessment for stakeholder adaptation planning in New York City. *J. Appl. Meteorol. Climatol.* **50**, 2247–2266 (2011).
7. Rosenzweig, C. & Solecki, W. D. *Climate Change and A Global City: The Potential Consequences of Climate Variability and Change: Metro East Coast: Executive Summary and Recommendations* (Columbia Earth Institute, 2001).
8. PlaNYC: A Greener, Greater New York (City of New York, 2007).
9. Dessai, S. Heat stress and mortality in Lisbon Part II. An assessment of the potential impacts of climate change. *Int. J. Biometeorol.* **48**, 37–44 (2003).
10. Peng, R. D., Bobb, J. F., Tebaldi, C., McDaniel, L., Bell, M. L. & Dominici, F. Toward a quantitative estimate of future heat wave mortality under global climate change. *Environ. Health Perspect.* **119**, 701–706 (2011).
11. Knowlton, K. *et al.* Projecting Heat-related mortality impacts under a changing climate in the New York city region. *Am. J. Publ. Health* **97**, 2028–2034 (2007).
12. Gosling, S. N., McGregor, G. R. & Lowe, J. A. Climate change and heat-related mortality in six cities Part 2: Climate model evaluation, sensitivity analysis, and estimation of future impacts. *Int. J. Biometeorol.* **53**, 31–51 (2009).
13. Sheridan, S. C. *et al.* Future heat vulnerability in California, Part II: Projecting future heat-related mortality. *Climatic Change* **115**, 311–325 (2012).
14. Ostro, B. *et al.* The impact of future summer temperature on public health in Barcelona and Catalonia, Spain. *Int. J. Biometeorol.* **56**, 1135–1144 (2012).
15. Langford, I. H. & Bentham, G. The potential effects of climate change on winter mortality in England and Wales. *Int. J. Biometeorol.* **38**, 141–147 (1995).
16. Doyon, B., Bélanger, D. & Gosselin, P. The potential impact of climate change on annual and seasonal mortality for three cities in Québec, Canada. *Int. J. Health Geogr.* **7**, 23 (2008).
17. Huang, C. *et al.* The impact of temperature on years of life lost in Brisbane, Australia. *Nature Clim. Change* **2**, 265–70 (2012).
18. Kalkstein, L. S. & Greene, J. S. An evaluation of climate/mortality relationships in large US cities and the possible impacts of a climate change. *Environ. Health Perspect.* **105**, 84–93 (1997).
19. Donaldson, G. C. *et al.* *Heat- and Cold-related Mortality and Morbidity and Climate Change. Health Effects of Climate Change in the UK* (Department of Health, 2001).
20. Guest, C. S. *et al.* Climate and mortality in Australia: Retrospective study, 1979–1990, and predicted impacts in five major cities in 2030. *Clim. Res.* **13**, 1–15 (1999).
21. Hayashi, A. *et al.* Evaluation of global warming impacts for different levels of stabilization as a step toward determination of the long-term stabilization target. *Climatic Change* **98**, 87–112 (2010).
22. Martin, S. L. *et al.* Climate change and future temperature-related mortality in 15 Canadian cities. *Int. J. Biometeorol.* **56**, 605–619 (2012).
23. Barnett, A. G. Temperature and cardiovascular deaths in the US elderly: Changes over time. *Epidemiology* **18**, 369–372 (2007).
24. Kalkstein, L. S. & Davis, R. E. Weather and human mortality: An evaluation of demographic and interregional responses in the United States. *Ann. Assoc. Am. Geogr.* **79**, 44–64 (1989).
25. Gasparrini, A., Armstrong, B. & Kenward, M. G. Distributed lag non-linear models. *Stat. Med.* **29**, 2224–2234 (2010).
26. Guo, Y. *et al.* The impact of temperature on mortality in Tianjin, China: A case-crossover design with a distributed lag non-linear model. *Environ. Health Perspect.* **119**, 1719–1725 (2011).
27. IPCC *Special Report on Emissions Scenarios* (eds Nakicenovic, N. & Swart, R.) (Cambridge Univ. Press, 2000).
28. Maurer, E. P., Brekke, L., Pruitt, T. & Duffy, P. B. Fine-resolution climate projections enhance regional climate change impact studies. *Eos. Trans. AGU* **88**, 504–504 (2007).
29. Grotch, S. L. & MacCracken, M. C. The use of general circulation models to predict regional climatic change. *J. Clim.* **4**, 286–303 (1991).
30. Ballester, J. *et al.* Changes in European temperature extremes can be predicted from changes in PDF central statistics. *Climatic Change* **98**, 277–284 (2010).

Acknowledgements

T.L. was supported by the National Natural Science Foundation of China (Project Number: 21277135, 40905069; 41110104015). R.M.H. and P.K. were supported by grant #NA10OAR4310212 from the US National Oceanic and Atmospheric Administration. P.K. was also supported by grant #P30 ES09089 from the US National Institute of Environmental Health Sciences. D. Bader assisted with technical aspects of the downscaling.

Author contributions

T.L. and P.K. contributed to the research design, data analysis and paper writing; R.M.H. designed and led the temperature downscaling work.

Additional information

Supplementary information is available in the [online version of the paper](#). Reprints and permissions information is available online at www.nature.com/reprints. Correspondence and requests for materials should be addressed to P.K.

Competing financial interests

The authors declare no competing financial interests.